

Exact emergent quantum state designs from quantum chaotic dynamics

Wen Wei Ho¹ and Soonwon Choi²

¹*Department of Physics, Stanford University, Stanford, CA 94305, USA*

²*Center for Theoretical Physics, Massachusetts Institute of Technology, Cambridge, MA 02139, USA*

(Dated: February 15, 2022)

We present exact results on a novel kind of emergent random matrix universality that quantum many-body systems at infinite temperature can exhibit. Specifically, we consider an ensemble of pure states supported on a small subsystem, generated from projective measurements of the remainder of the system in a local basis. We rigorously show that the ensemble, derived for a class of quantum chaotic systems undergoing quench dynamics, approaches a universal form completely independent of system details: it becomes uniformly distributed in Hilbert space. This goes beyond the standard paradigm of quantum thermalization, which dictates that the subsystem relaxes to an ensemble of quantum states that reproduces the expectation values of local observables in a thermal mixed state. Our results imply more generally that the *distribution* of quantum states themselves becomes indistinguishable from those of uniformly random ones, i.e. the ensemble forms a *quantum state-design* in the parlance of quantum information theory. Our work establishes bridges between quantum many-body physics, quantum information and random matrix theory, by showing that pseudo-random states can arise from isolated quantum dynamics, opening up new ways to design applications for quantum state tomography and benchmarking.

Introduction. Universality, the emergence of features independent of precise microscopic details, allows us to simplify the analysis of complex systems and to establish important general principles. Quantum thermalization prescribes a scenario where such universal behavior arises from generic dynamics of isolated quantum many-body systems. It is widely accepted that quantum chaotic many-body systems – that is, systems with spectral correlations described by random matrix theory (RMT) [1, 2] – will locally relax to maximally entropic thermal states constrained only by global conservation laws [3]. Physically, this arises because of the extensive amounts of entanglement generated between a local subsystem and its complement, which acts like a bath. Ignoring the state of the bath, the subsystem acquires a universal, mixed form, described by a generalized Gibbs state. Understanding this universality has led to the development of the eigenstate thermalization hypothesis (ETH) [4, 5], and has also spurred intense research into mechanisms for its break-down such as many-body localization [3, 6] and quantum many-body scarring [7, 8].

Here we take a perspective different from the standard treatment of quantum thermalization and ask: what happens if (some) information about the bath is explicitly kept track of instead of discarded – how then does one describe properties of a local subsystem? Will there be any kind of universality in this setting? Such a consideration is of fundamental interest, as it would illuminate the role of the bath in quantum thermalization beyond the conventional paradigm. It is also natural given the capability of present-day quantum simulators, which allow access to correlations not only within a subsystem, but also *between* the subsystem and its complement.

To this end we consider here the *projected ensemble*, introduced in Refs. [9, 10]. This is a collection of *pure*

states supported on a local subsystem A , each of which is associated with the outcome of a projective measurement of the complementary subsystem B in a fixed local basis. Such an ensemble contains strictly more information than the conventionally studied reduced density matrix ρ_A , which is recovered from the first moment of the ensemble’s distribution; higher moments further characterize statistical properties of the ensemble in increasingly refined fashions, such as the spread of projected states over Hilbert space.

In this Letter, we present exact results on universal properties exhibited by the projected ensemble, obtained from a class of quantum chaotic many-body dynamics without global conservation laws: we rigorously show that its statistics becomes completely independent of microscopic details over time. Concretely, we focus on the non-integrable, periodically-kicked Ising model and prove in the thermodynamic limit (TDL) that the projected ensemble evolves toward a maximally entropic distribution, i.e. all its moments agree *exactly* with those of the uniform ensemble over Hilbert space. In the parlance of quantum information theory (QIT), such an ensemble is said to form a *quantum state-design* [11–14]. Intriguingly, this happens in finite time in quench dynamics.

Our results demonstrate a new kind of emergent random matrix universality exhibited by quantum chaotic many-body systems at infinite temperature: at late times, a local subsystem A is characterized by an ensemble of states indistinguishable from random ones not only within expectation values of observables (à la standard quantum thermalization [3]), but also within *any* statistical properties of the states themselves. In other words, there is no protocol performable on A which can information-theoretically differentiate the projected states from uniformly random ones. Theoretical and ex-

perimental evidence have been conjecturing the appearance of such universality across wide classes of physical systems and states [9, 10]; our results complement these by furnishing an exactly-solvable model where this conjecture can be proven.

We note that the kicked Ising model we study exhibits RMT spectral statistics for all times, as proven in [15]; the result involved a necessary averaging over a small but non-vanishing amount of disorder. In contrast, our work demonstrates how universal randomness can also arise naturally within dynamics of a single instance of a clean Hamiltonian and wavefunction, induced by measurements.

Projected ensembles and quantum state-designs. The projected ensemble is defined as follows [9, 10]. Consider a single generator state $|\Psi\rangle$ of a large system of N qubits (generalization to a qudit system is immediate), and a bipartition into subsystems A and B with N_A and N_B qubits respectively. We assume the state of B is projectively measured in the local computational basis, so that one obtains a bit-string outcome $z_B = (z_{B,1}, z_{B,2}, \dots, z_{B,N_B}) \in \{0, 1\}^{N_B}$ and its associated *pure* quantum state on A

$$|\psi(z_B)\rangle = (\mathbb{I}_A \otimes \langle z_B |) |\Psi\rangle / \sqrt{p(z_B)} \quad (1)$$

with probability $p(z_B) = \langle \Psi | \mathbb{I}_A \otimes |z_B\rangle \langle z_B | \Psi \rangle$, see Fig. 1a. The set of (generally non-orthogonal) projected states over all 2^{N_B} outcomes with respective probabilities, forms the *projected ensemble* $\mathcal{E} := \{p(z_B), |\psi(z_B)\rangle\}$.

The statistical properties of \mathcal{E} is characterized by moments of its distribution. Concretely, the k -th moment is captured by a density matrix

$$\rho_{\mathcal{E}}^{(k)} = \sum_{z_B} p(z_B) (|\psi(z_B)\rangle \langle \psi(z_B)|)^{\otimes k} \quad (2)$$

acting on the k -fold tensor product space $\mathcal{H}_A^{\otimes k}$, where \mathcal{H}_A is the Hilbert space of A . The first moment $k=1$ (mean) contains information about the expectation value of any physical observable in A , as $\rho_{\mathcal{E}}^{(1)}$ equals ρ_A . Higher moments $k \geq 2$ capture properties beyond, in particular quantifying the variance, skewness, etc. of the distribution of projected states over \mathcal{H}_A . We note that understanding statistical properties of ensembles of quantum states or unitaries (specifically quantifying the degree of randomness) forms the basis of many applications in quantum information science such as cryptography, tomography, or machine learning, as well as sampling-based computational-advantage tests for near-term quantum devices [16–29]. Eq. (2) probes analogous information for the projected states of a small subsystem, where now the ensemble is of states correlated to measurement outcomes of the bath. We emphasize such higher moments have begun to be experimentally probed in quantum simulators [9], highlighting the need to better understand their universal properties.

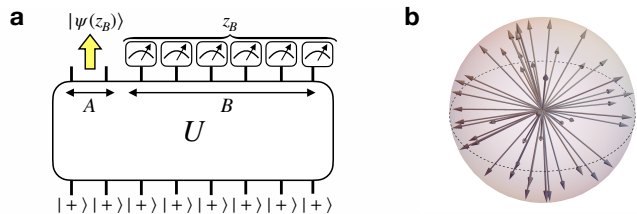


Figure 1. (a) Projected state $|\psi(z_B)\rangle$ on A arises from a projective measurement of subsystem B in the local z -basis, with measurement outcome z_B . Here the generator state is an initial product state $|+\rangle^{\otimes N}$ evolved by unitary U . (b) Distribution over Hilbert space of projected states $|\psi(z_B)\rangle$, each occurring with probability $p(z_B)$, illustrated for $N_A = 1$. The projected ensemble \mathcal{E} forming a quantum state-design in the TDL implies the states cover the Bloch sphere uniformly.

We focus in this paper on generator states arising from quench dynamics of systems without explicit conservation laws. As quantum thermalization dictates that the first moment should acquire a universal form $\rho_{\mathcal{E}}^{(1)} \propto \mathbb{I}_A$ over time, it is natural to conjecture that higher moments become similarly ‘maximally-mixed’ [9, 10]. To quantify this, we appeal to the notion of *quantum state-designs* in QIT [11–14], which measures the similarity of \mathcal{E} to an ensemble of uniformly (i.e. Haar)-random states on A [30], whose k -th moment is given by

$$\rho_{\text{Haar}}^{(k)} = \int_{\psi \sim \text{Haar}(2^{N_A})} d\psi (|\psi\rangle \langle \psi|)^{\otimes k}. \quad (3)$$

The agreement of moments is captured by the trace distance $\Delta^{(k)} = \frac{1}{2} \|\rho_{\mathcal{E}}^{(k)} - \rho_{\text{Haar}}^{(k)}\|_1$; if $\Delta^{(k)}$ vanishes (is ϵ -small), then \mathcal{E} is said to form an exact (ϵ -approximate) quantum state k -design. Below, we study a local, quantum chaotic model where the projected ensemble from quench dynamics can be exactly calculated, and analyze the degree to which state k -designs are formed, with time and number of qubits measured.

Model and results. We consider a 1D chain of N spin-1/2 particles (or qubits) evolving under dynamics generated by the Floquet unitary

$$U_F = U_h e^{-iH_{\text{Ising}}\tau}. \quad (4)$$

Here $U_h = \exp(-ih \sum_{i=1}^N \sigma_i^y)$ is a global y -rotation, while $H_{\text{Ising}} = J \sum_{i=1}^{N-1} \sigma_i^z \sigma_{i+1}^z + g \sum_{i=1}^N \sigma_i^z + (b_1 \sigma_1^z + b_N \sigma_N^z)$ is the Ising model with nearest-neighbor interaction strength J and longitudinal field g , applied for time $\tau = 1$. $\sigma_i^x, \sigma_i^y, \sigma_i^z$ are standard Pauli matrices at site i . The last term in H_{Ising} are boundary terms with strengths we fix to $b_1 = b_N = \pi/4$, introduced solely for technical simplifications. See [30] for discussions of the case with periodic boundary conditions.

Equation (4) describes unitary evolution by a 1D periodically-kicked Ising model, which is known to be non-integrable for generic values of (J, h, g) , and possesses no global conservation laws. We fix $J, h = \pi/4$ and

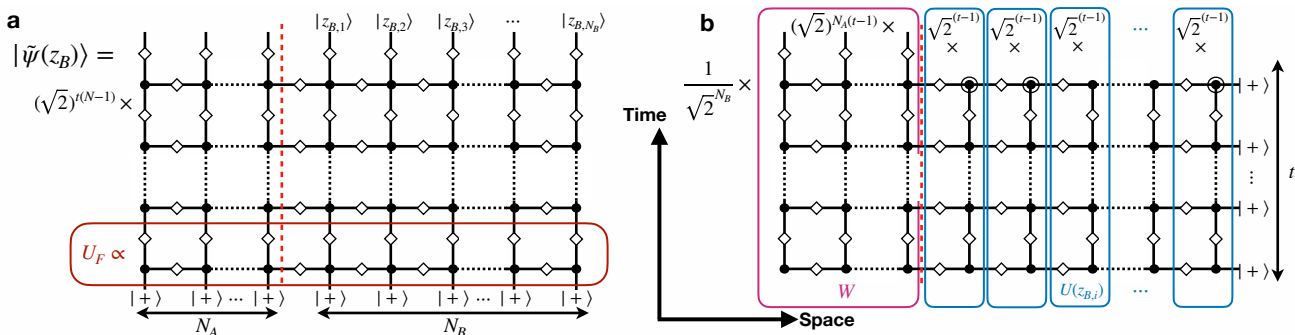


Figure 2. (a) Tensor-network representation of (unnormalized) projected state $|\tilde{\psi}(z_B)\rangle$ for the kicked Ising model, given measurement outcome z_B . Each black node carries factor g , see Eq. (5). The red box is proportional to the Floquet unitary U_F , which acts on the spin chain with initial state $|+\rangle^{\otimes N}$. There are t applications of U_F . (b) The same state can be obtained from evolution in the spatial direction (right to left) of the initial state $|+\rangle^{\otimes t}$ on the ‘dual chain’, by products of unitaries $U(z_{B,i})$ (blue box) where $z_{B,i} \in \{0, 1\}$, illustrated here as the particular product $U(1)U(1)U(0)\cdots U(1)$. $U(z_{B,i})$ is generated also by a kicked Ising model; however the strength of the longitudinal field at temporal site t depends on $z_{B,i}$ (see main text). There is a final linear map W (pink box) sending the resulting t -qubit state to a state supported on A .

allow arbitrary g excluding exceptional points $g \notin \mathbb{Z}\pi/8$. We calculate the projected ensemble \mathcal{E} on subsystem A comprised of the first N_A contiguous qubits, measuring the remaining N_B qubits in the computational z -basis from the generator state $|\Psi(t)\rangle = U_F^t |+\rangle^{\otimes N}$, where $|+\rangle$ is the x -polarized state (see [30] for a discussion on other initial states). Here $t \in \mathbb{Z}$ is the number of applications of U_F .

Our central result is that for a fixed subsystem A , evolution under the kicked Ising model for a sufficiently long but finite time followed by measurements on an infinitely-large complementary subsystem B , essentially effects random rotations on A , so that the projected states are statistically indistinguishable from Haar-random ones, see Fig. 1b. Precisely, we have:

Theorem 1. *For $t \geq N_A$ and $g \notin \mathbb{Z}\pi/8$, the projected ensemble \mathcal{E} forms an exact quantum state-design in the thermodynamic limit: for any k , $\lim_{N_B \rightarrow \infty} \rho_{\mathcal{E}}^{(k)} = \rho_{\text{Haar}}^{(k)}$.*

The proof of our claim combines several tools used in quantum chaos and QIT, outlined here. First, we leverage a so-called *dual-unitary* property of U_F enjoyed at the special values of J, h picked [15, 31]: the unitary represented as a tensor-network can be interpreted as unitary evolution not only along the temporal, but also the *spatial*-direction (Fig. 2). In the dual picture, measuring N_B qubits induces an ensemble of quantum circuits enumerated by measurement outcomes, which act on t fictitious qubits. Each projected state (1) arises from a particular circuit evolution, followed by a map to the space of N_A qubits [discussed in Eq. (7)]. We show the ensemble of circuits, when infinitely-deep (corresponding to the TDL), is statistically indistinguishable from Haar-random unitaries – i.e. it forms a *unitary* design [11–14], allowing us to establish that the projected states are correspondingly uniformly distributed over Hilbert space.

We now flesh out the above steps. We first introduce

the following elementary diagrams:

$$\diamond = \frac{1}{\sqrt{2}} \begin{pmatrix} 1 & 1 \\ 1 & -1 \end{pmatrix}, \quad \begin{array}{c} z_1 \\ \nearrow \\ \text{---} \\ \searrow \\ z_2 \end{array} \begin{array}{c} z_3 \\ \nearrow \\ \text{---} \\ \searrow \\ z_2 \end{array} = \delta_{z_1 z_2 z_3} e^{-ig(1-2z_1)}. \quad (5)$$

The former represents the Hadamard gate, while the latter is a tensor evaluating to non-zero values, $e^{\mp ig}$, if and only if all three indices $z_i \in \{0, 1\}$ agree, $z_1, z_2, z_3 = 0(1)$, respectively. These tensors can be contracted with one another, or with quantum states (see [30] for details). Using this notation, evolution by Ising interactions and transverse fields can be cast (up to irrelevant global phases) as

$$e^{-i\frac{\pi}{4}\sigma^z \otimes \sigma^z} = \sqrt{2} \times \begin{array}{c} \pi/4 \\ \text{---} \\ \text{---} \\ \pi/4 \end{array}, \quad e^{-i\frac{\pi}{4}\sigma^y} = \begin{array}{c} \pi/2 \\ \text{---} \\ \text{---} \end{array}. \quad (6)$$

Additionally, a measurement at site i is represented by a contraction with an outcome state $|z_{B,i}\rangle$, yielding two possibilities

$$\begin{array}{c} \text{---} \\ \text{---} \\ \text{---} \\ \text{---} \end{array} \begin{array}{c} z_{B,i} \\ \nearrow \\ \text{---} \\ \searrow \\ \text{---} \end{array} = \begin{cases} \begin{array}{c} \text{---} \\ \text{---} \\ \text{---} \\ \text{---} \end{array} \begin{array}{c} g \\ \nearrow \\ \text{---} \\ \searrow \\ \text{---} \end{array} |+\rangle & \text{if } z_{B,i} = 0, \\ \begin{array}{c} \text{---} \\ \text{---} \\ \text{---} \\ \text{---} \end{array} \begin{array}{c} g+\pi/2 \\ \nearrow \\ \text{---} \\ \searrow \\ \text{---} \end{array} |+\rangle & \text{if } z_{B,i} = 1. \end{cases}$$

Combined together, our diagrams allow a particularly compact tensor-network representation of the (unnormalized) projected state $|\tilde{\psi}(z_B)\rangle = (\mathbb{I}_A \otimes \langle z_B|) U_F^t |+\rangle^{\otimes N}$ (Fig. 2a). We note this tensor-network state is closely related to the one representing the 2D cluster state which forms a universal resource for measurement-based quantum computation [30, 32].

Figure 2a demonstrates the dual-unitary property of U_F evidently: there is a self-similarity of the diagram read bottom-up (temporally) or right-left (spatially). Precisely, Fig. 2b illustrates $|\tilde{\psi}(z_B)\rangle$ can be equivalently interpreted as evolution of an initial state $|+\rangle^{\otimes t}$ on t qubits (‘dual chain’) by quantum circuits $\mathcal{U}(z_B) := U(z_{B,1})U(z_{B,2})\cdots U(z_{B,N_B})$, followed by a linear map W transforming the resulting state to one on

N_A qubits:

$$|\tilde{\psi}(z_B)\rangle = \frac{1}{\sqrt{2^{N_B}}} WU(z_B)|+\rangle^{\otimes t}. \quad (7)$$

Here, $U(z_{B,i})$ takes two forms: $U(0), U(1)$, depending on the measurement outcome $z_{B,i} \in \{0, 1\}$. Both are identical in form and have parameters J, h, g, b_1 similar to the Floquet unitary (4), upon interpreting the site index i to run along the t -site dual chain, except with differing boundary fields $b_t = \pi/4(3\pi/4)$ if $z_{B,i} = 0(1)$. Eq. (2) can thus be rewritten as a sum over all circuit evolutions:

$$\rho_{\mathcal{E}}^{(k)} = \sum_{z_B} \frac{1}{2^{N_B}} \frac{(WU(z_B)(|+\rangle\langle +|)^{\otimes t}U(z_B)^\dagger W^\dagger)^{\otimes k}}{(\langle +|^{\otimes t}U(z_B)^\dagger W^\dagger WU(z_B)|+\rangle^{\otimes t})^{k-1}}. \quad (8)$$

We now observe that for $t \geq N_A$, W is expressible as $W = \sqrt{2^{(t-N_A)}} \langle +|^{\otimes(t-N_A)} V$ [33], where V is a unitary on \mathbb{C}^{2^t} whose particular form is unimportant as we will argue below. This assertion can be straightforwardly verified diagrammatically [30]. We further observe that Eq. (8) can be thought of as the average behavior of a function taking as input a circuit $\mathcal{U}(z_B)$, with output $\frac{(\dots)^{\otimes k}}{(\dots)^{k-1}}$, sampled *uniformly* over all 2^{N_B} possible circuits indexed by z_B . Our task therefore falls to examining the statistics of the (uniform) ensemble of *unitaries* $\mathcal{E}_{\mathcal{U}} := \{\mathcal{U}(z_B)\}$. We show that this discrete set $\mathcal{E}_{\mathcal{U}}$ in fact samples the (continuous) space of unitaries on \mathbb{C}^{2^t} uniformly in the TDL $N_B \rightarrow \infty$, stated in Theorem 2 below.

We can thus in Eq. (8) replace in the TDL the sum over states $\mathcal{U}(z_B)|+\rangle^{\otimes t}$, which by virtue of Theorem 2 become uniformly distributed over Hilbert-space, with an integral over Haar-random states. This step is justified more rigorously in [30]. The unitary V entering in the decomposition of W can then be absorbed in the integral via invariance of the Haar measure, leading to

$$\lim_{N_B \rightarrow \infty} \rho_{\mathcal{E}}^{(k)} = \int_{\Psi \sim \text{Haar}(2^t)} d\Psi \frac{(|\Psi_+\rangle\langle \Psi_+|)^{\otimes k}}{\langle \Psi_+ | \Psi_+ \rangle^k} \times 2^{t-N_A} \langle \Psi_+ | \Psi_+ \rangle,$$

where $|\Psi_+\rangle = \langle +|^{\otimes(t-N_A)} |\Psi\rangle$. Finally, Lemma 4 of [10] specifies that random variables $\frac{(|\Psi_+\rangle\langle \Psi_+|)^{\otimes k}}{\langle \Psi_+ | \Psi_+ \rangle^k}$ and $2^{t-N_A} \langle \Psi_+ | \Psi_+ \rangle$ are independent, allowing us to distribute the integral: the former equals (3) while the latter evaluates to 1, giving our claimed result. ■

Figure 3 numerically illustrates the emergence of quantum state-designs for various Floquet times and projected subsystem size N_B . We find that \mathcal{E} forms an exact state k -design for $k=1$ when $N_B \geq N_A = t$ (i.e. reduced density matrix is maximally mixed), as expected from the results of [34], while it converges exponentially fast with N_B for higher ks .

Statistics of unitary ensemble $\mathcal{E}_{\mathcal{U}}$. In Theorem 1, we used the following nontrivial result describing the distribution of unitaries $\mathcal{U}(z_B)$ in the TDL:

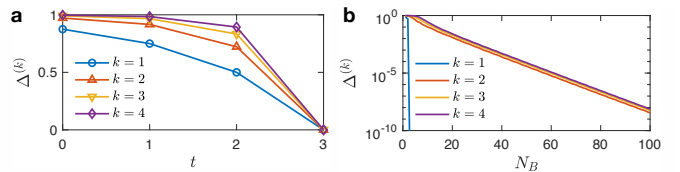


Figure 3. Trace distance $\Delta^{(k)}$ of k -th moment of projected ensemble to a Haar random ensemble versus (a) time and (b) projected subsystem size N_B , for $g = \pi/9$ and $N_A = 3$. For (a), $N_B = 100$. For (b), $t = N_A = 3$.

Theorem 2. For $g \notin \mathbb{Z}\pi/8$, all moments k of $\mathcal{E}_{\mathcal{U}}$ and the Haar-random unitary ensemble agree in the TDL: $\lim_{N_B \rightarrow \infty} \sum_{z_B} \frac{1}{2^{N_B}} \mathcal{U}(z_B)^{\otimes k} \otimes \mathcal{U}(z_B)^{* \otimes k} = \int_{U \sim \text{Haar}(2^t)} dU U^{\otimes k} \otimes U^{* \otimes k}$. That is, $\mathcal{E}_{\mathcal{U}}$ in the TDL forms an exact unitary-design.

Recall an element of $\mathcal{E}_{\mathcal{U}}$ is a quantum circuit e.g. $U(1)U(0)U(0)U(1)\dots$, which is interpretable as an instance of evolution by a *randomly-kicked Ising model* on t qubits, where the randomness arises only from the boundary longitudinal field at site t taking two possible values g and $g + \pi/2$ with equal probability, between every kick. Thus, Theorem 2 amounts to saying that unitaries generated by a kicked Ising model with time-dependent but ultra-localized randomness, suffice to form arbitrarily good approximations of Haar-random unitaries after long enough times. In contrast, many previous works concerning the emergence of such unitary-designs in dynamics assume *global* (i.e. an extensive number of) system parameters that are random in time [18, 35, 36], and so the randomly-kicked Ising model constitutes an example where the degree of randomness required is arguably minimal. The proof of Theorem 2, presented in [30], is technical, but essentially amounts to showing that basic unitaries $U(0), U(1)$ (and their inverses) form a universal gate set, such that any unitary on \mathbb{C}^{2^t} can be reached from their products [37].

Discussion. Our main result, Theorem 1, establishes the first provable example of a new kind of emergent random matrix universality exhibited by quantum chaotic many-body systems, conjectured by [9, 10]. It represents a deep form of quantum thermalization characterized by a maximally entropic distribution of pure states of a subsystem induced by the bath, suggesting a generalization of the ETH to account for such features. An open question is how such universality is modified in the presence of globally-conserved quantities, like energy. For $k=1$, quantum thermalization already specifies a universal form at late-times: a Gibbs ensemble at a definite temperature. What are the universal ensembles, if any, that $\rho_{\mathcal{E}}^{(k)}$ for $k \geq 2$ tend toward? From a technical standpoint, our work asserts the projected ensemble forms a quantum state-design in the limit when infinitely-many qubits are measured; understanding the rate of convergence with large but finite system-sizes would be very interesting (see [30] for a preliminary discussion).

The appearance of quantum state-designs in a physical system has also quantum information science applications, in particular for tasks like state-tomography, benchmarking, or cryptography, which employ ensembles of random unitaries or states [16–29, 38]. For example, by applying random unitaries, projectively measuring, and processing the classical data, one can in certain cases reconstruct an approximate description of a system’s state in a protocol called classical shadow tomography [26]. Our results suggest that one can replace the direct application of a random unitary, which requires fine-control, with simple projective measurements following quantum chaotic dynamics to effectively realize random rotations on a subsystem, potentially amounting to a hardware-efficient method to implement the tomographic protocol.

Acknowledgments. We thank N. Hunter-Jones, H. Pichler and X.-L. Qi for useful discussions. We also thank J. Cotler and N. Maskara for a careful read of the manuscript. W. W. Ho is supported in part by the Stanford Institute of Theoretical Physics.

-
- [1] M. L. Mehta, *Random Matrices and the Statistical Theory of Energy Levels* (Academic Press, 1967).
- [2] F. Haake, *Quantum Signatures of Chaos* (Springer, 2001).
- [3] Rahul Nandkishore and David A. Huse, “Many-body localization and thermalization in quantum statistical mechanics,” *Annual Review of Condensed Matter Physics* **6**, 15–38 (2015).
- [4] J. M. Deutsch, “Quantum statistical mechanics in a closed system,” *Phys. Rev. A* **43**, 2046–2049 (1991).
- [5] Mark Srednicki, “Chaos and quantum thermalization,” *Phys. Rev. E* **50**, 888–901 (1994).
- [6] Dmitry A. Abanin, Ehud Altman, Immanuel Bloch, and Maksym Serbyn, “Colloquium: Many-body localization, thermalization, and entanglement,” *Rev. Mod. Phys.* **91**, 021001 (2019).
- [7] Maksym Serbyn, Dmitry A. Abanin, and Zlatko Papić, “Quantum many-body scars and weak breaking of ergodicity,” *Nature Physics* **17**, 675–685 (2021).
- [8] Sanjay Moudgalya, B. Andrei Bernevig, and Nicolas Regnault, “Quantum Many-Body Scars and Hilbert Space Fragmentation: A Review of Exact Results,” arXiv e-prints, arXiv:2109.00548 (2021), arXiv:2109.00548 [cond-mat.str-el].
- [9] Joonhee Choi, Adam L. Shaw, Ivaylo S. Madjarov, Xin Xie, Jacob P. Covey, Jordan S. Cotler, Daniel K. Mark, Hsin-Yuan Huang, Anant Kale, Hannes Pichler, Fernando G. S. L. Brandão, Soonwon Choi, and Manuel Endres, “Emergent Randomness and Benchmarking from Many-Body Quantum Chaos,” arXiv e-prints, arXiv:2103.03535 (2021), arXiv:2103.03535 [quant-ph].
- [10] Jordan S. Cotler, Daniel K. Mark, Hsin-Yuan Huang, Felipe Hernandez, Joonhee Choi, Adam L. Shaw, Manuel Endres, and Soonwon Choi, “Emergent quantum state designs from individual many-body wavefunctions,” arXiv e-prints, arXiv:2103.03536 (2021), arXiv:2103.03536 [quant-ph].
- [11] D.P. DiVincenzo, D.W. Leung, and B.M. Terhal, “Quantum data hiding,” *IEEE Transactions on Information Theory* **48**, 580–598 (2002).
- [12] A. Ambainis and J. Emerson, “Quantum t-designs: t-wise independence in the quantum world,” in *2007 22nd Annual IEEE Conference on Computational Complexity* (IEEE Computer Society, Los Alamitos, CA, USA, 2007) pp. 129–140.
- [13] D. Gross, K. Audenaert, and J. Eisert, “Evenly distributed unitaries: On the structure of unitary designs,” *Journal of Mathematical Physics* **48**, 052104 (2007), <https://doi.org/10.1063/1.2716992>.
- [14] Daniel A. Roberts and Beni Yoshida, “Chaos and complexity by design,” *Journal of High Energy Physics* **2017** (2017), 10.1007/jhep04(2017)121.
- [15] Bruno Bertini, Pavel Kos, and Tomaž Prosen, “Exact spectral form factor in a minimal model of many-body quantum chaos,” *Phys. Rev. Lett.* **121**, 264101 (2018).
- [16] E. Knill, D. Leibfried, R. Reichle, J. Britton, R. B. Blakestad, J. D. Jost, C. Langer, R. Ozeri, S. Seidelin, and D. J. Wineland, “Randomized benchmarking of quantum gates,” *Phys. Rev. A* **77**, 012307 (2008).
- [17] Easwar Magesan, J. M. Gambetta, and Joseph Emerson, “Scalable and robust randomized benchmarking of quantum processes,” *Phys. Rev. Lett.* **106**, 180504 (2011).
- [18] Fernando G. S. L. Brandão, Aram W. Harrow, and Michał Horodecki, “Efficient quantum pseudorandomness,” *Phys. Rev. Lett.* **116**, 170502 (2016).
- [19] Gorjan Alagic, Tommaso Gagliardoni, and Christian Majenz, “Unforgeable quantum encryption,” in *Advances in Cryptology – EUROCRYPT 2018*, edited by Jesper Buus Nielsen and Vincent Rijmen (Springer International Publishing, Cham, 2018) pp. 489–519.
- [20] Adam Bouland, Bill Fefferman, Chinmay Nirkhe, and Umesh Vazirani, “On the complexity and verification of quantum random circuit sampling,” *Nature Physics* **15**, 159–163 (2018).
- [21] J. Haferkamp, D. Hangleiter, A. Bouland, B. Fefferman, J. Eisert, and J. Bermejo-Vega, “Closing gaps of a quantum advantage with short-time hamiltonian dynamics,” *Phys. Rev. Lett.* **125**, 250501 (2020).
- [22] P. Sen, “Random measurement bases, quantum state distinction and applications to the hidden subgroup problem,” in *21st Annual IEEE Conference on Computational Complexity (CCC’06)* (2006) pp. 14 pp.–287.
- [23] Patrick Hayden, Debbie Leung, Peter W. Shor, and Andreas Winter, “Randomizing quantum states: Constructions and applications,” *Communications in Mathematical Physics* **250**, 371–391 (2004).
- [24] M. Oszmaniec, R. Augusiak, C. Gogolin, J. Kołodyński, A. Acín, and M. Lewenstein, “Random bosonic states for robust quantum metrology,” *Phys. Rev. X* **6**, 041044 (2016).
- [25] Shelby Kimmel and Yi-Kai Liu, “Phase retrieval using unitary 2-designs,” *2017 International Conference on Sampling Theory and Applications (SampTA)* (2017), 10.1109/sampta.2017.8024414.
- [26] Hsin-Yuan Huang, Richard Kueng, and John Preskill, “Predicting many properties of a quantum system from very few measurements,” *Nature Physics* **16**, 1050–1057 (2020).
- [27] Yoshifumi Nakata, Da Zhao, Takayuki Okuda, Eiichi Bannai, Yasunari Suzuki, Shiro Tamiya, Kentaro Heya, Zhiguang Yan, Kun Zuo, Shuhei Tamate, Yu-

- taka Tabuchi, and Yasunobu Nakamura, “Quantum circuits for exact unitary t -designs and applications to higher-order randomized benchmarking,” (2021), [arXiv:2102.12617 \[quant-ph\]](#).
- [28] Dorit Aharonov, Jordan Cotler, and Xiao-Liang Qi, “Quantum Algorithmic Measurement,” arXiv e-prints, [arXiv:2101.04634](#) (2021), [arXiv:2101.04634 \[quant-ph\]](#).
- [29] Hsin-Yuan Huang, Richard Kueng, and John Preskill, “Information-theoretic bounds on quantum advantage in machine learning,” *Phys. Rev. Lett.* **126**, 190505 (2021).
- [30] See Supplemental material online for details of statements and proofs presented in the main text, which includes Refs. [10, 14, 15, 32, 34, 39–41].
- [31] M Akila, D Waltner, B Gutkin, and T Guhr, “Particle-time duality in the kicked ising spin chain,” *Journal of Physics A: Mathematical and Theoretical* **49**, 375101 (2016).
- [32] Robert Raussendorf and Hans J. Briegel, “A one-way quantum computer,” *Phys. Rev. Lett.* **86**, 5188–5191 (2001).
- [33] I.e. W is proportional to an isometry, $WW^\dagger \propto \mathbb{I}_{2^{N_A}}$.
- [34] Bruno Bertini, Pavel Kos, and Tomaž Prosen, “Entanglement spreading in a minimal model of maximal many-body quantum chaos,” *Phys. Rev. X* **9**, 021033 (2019).
- [35] Fernando G. S. L. Brandão, Aram W. Harrow, and Michał Horodecki, “Local random quantum circuits are approximate polynomial-designs,” *Communications in Mathematical Physics* **346**, 397–434 (2016).
- [36] Yoshifumi Nakata, Christoph Hirche, Masato Koashi, and Andreas Winter, “Efficient quantum pseudorandomness with nearly time-independent hamiltonian dynamics,” *Phys. Rev. X* **7**, 021006 (2017).
- [37] A result by [42] further guarantees such products when infinitely-long become uniformly distributed over the unitary group, though we do not use this in our proof.
- [38] Frank Arute, Kunal Arya, Ryan Babbush, Dave Bacon, Joseph C. Bardin, Rami Barends, Rupak Biswas, Sergio Boixo, Fernando G. S. L. Brandao, David A. Buell, and et al., “Quantum supremacy using a programmable superconducting processor,” *Nature* **574**, 505–510 (2019).
- [39] R. Goodman and N. R. Wallach, *Representations and Invariants of the Classical Groups* (Cambridge University Press, 1998).
- [40] Iman Marvian and Robert W. Spekkens, “A generalization of schur–weyl duality with applications in quantum estimation,” *Communications in Mathematical Physics* **331**, 431–475 (2014).
- [41] J. Preskill, “Caltech lecture notes for physics 219/computer science 219 quantum computation course,” (2020), <http://theory.caltech.edu/preskill/ph229/notes/chap6.pdf>.
- [42] Joseph Emerson, Etera Livine, and Seth Lloyd, “Convergence conditions for random quantum circuits,” *Phys. Rev. A* **72**, 060302 (2005).

Supplemental material for: Exact emergent quantum state designs from quantum chaotic dynamics

Wen Wei Ho¹ and Soonwon Choi²

¹*Department of Physics, Stanford University, Stanford, CA 94305, USA*

²*Center for Theoretical Physics, Massachusetts Institute of Technology, Cambridge, MA 02139, USA*

(Dated: February 15, 2022)

In this supplemental material, we provide details on statements and theorems of the main paper. Section I elaborates on moments of an ensemble of Haar-random states. Section II discusses extensions of our results for the case of other initial states and the kicked Ising model with periodic boundary conditions. Section III presents some useful relations involving the basic diagrams used to represent the Floquet unitary as a tensor network. Section IV expounds on the comment made in the main text on the connection of the 1D kicked Ising unitary to the 2D cluster state, a universal resource for measurement-based quantum computation. Section V provides a diagrammatic proof of the decomposition of the linear map W asserted in the main text. Section VI presents additional details on the proof of Theorem 1, that the projected ensemble of the kicked Ising model (with open boundary conditions) forms a quantum state-design in the thermodynamic limit. Section VII presents the proof of Theorem 2, that the ensemble of unitaries \mathcal{E}_U forms a unitary-design in the thermodynamic limit. Section VIII discusses, in brief, the parameter governing how quickly the projected ensemble forms a quantum state-design as a function of system size. Section IX collects some technical lemmas used in the proof of Theorem 2.

I. MOMENTS OF AN ENSEMBLE OF HAAR-RANDOM STATES

By the Schur-Weyl duality [1–3], we can express the k -th moment of an ensemble of Haar random states on a d -dimensional Hilbert space \mathcal{H} as a uniform sum of permutation operators on $\mathcal{H}^{\otimes k}$:

$$\rho_{\text{Haar}}^{(k)} = \int_{\psi \sim \text{Haar}(d)} d\psi (|\psi\rangle\langle\psi|)^{\otimes k} = \frac{\sum_{\pi \in S_k} P(\pi)}{d(d+1)\cdots(d+k-1)}. \quad (\text{S1})$$

Here $P(\pi)$ is an operator acting on $\mathcal{H}^{\otimes k}$, which permutes the k copies of the Hilbert space \mathcal{H} according to a member π of the permutation group S_k on k elements:

$$P(\pi)|i_1, i_2, \dots, i_k\rangle = |i_{\pi(1)}, i_{\pi(2)}, \dots, i_{\pi(k)}\rangle, \quad (\text{S2})$$

where $1 \leq i \leq d$. Note that Eq. (S1) can also be written

$$\rho_{\text{Haar}}^{(k)} = \frac{\Pi_{\text{symm}}^{(k)}}{\binom{d+k-1}{k}} \quad (\text{S3})$$

where $\Pi_{\text{symm}}^{(k)}$ is the projector onto the symmetric subspace of $\mathcal{H}^{\otimes k}$. In the main text, we worked with $\mathcal{H} = \mathbb{C}^{2^{N_A}}$ as we considered the projected ensemble on a subsystem A of N_A qubits, so $d = 2^{N_A}$.

II. EXTENSIONS OF RESULTS

In the main text, we considered unitary dynamics by the 1D kicked Ising model on N qubits

$$U_F = U_h e^{-iH_{\text{Ising}}\tau}, \quad (\text{S4})$$

where

$$U_h = \exp\left(-ih \sum_{i=1}^N \sigma_i^y\right),$$

$$H_{\text{Ising}} = J \sum_{i=1}^{N-1} \sigma_i^z \sigma_{i+1}^z + g \sum_{i=1}^N \sigma_i^z + (b_1 \sigma_1^z + b_N \sigma_N^z). \quad (\text{S5})$$

The parameters used were $\tau = 1$, $(J, h, b_1, b_N) = (\pi/4, \pi/4, \pi/4, \pi/4)$, with arbitrary g as long as it stayed away from exceptional points $g \notin \mathbb{Z}\pi/8$. As written above, the model is defined on a chain with open boundary conditions.

Our central result (Theorem 1) was that the projected ensemble \mathcal{E} on a subsystem A , generated from a time-evolved wavefunction $|\Psi(t)\rangle = U_F^t |+\rangle^{\otimes N}$, forms an exact quantum state design in the thermodynamic limit, for Floquet times $t \geq N_A$. Precisely, the bipartition is such that subsystem A consists of the first N_A contiguous qubits while subsystem B the remaining qubits; the thermodynamic limit is taken as $N_B \rightarrow \infty$, keeping N_A fixed. We proved this leveraging the dual-unitary nature of the Floquet unitary U_F : written as a tensor network, it can be interpreted as unitary evolution not only along the standard time direction, but also along the spatial direction, acting on a ‘dual chain’ of t qubits. Measurements of N_B out of N qubits induce an ensemble of depth- N_B quantum circuits acting on the dual chain with initial state $|+\rangle^{\otimes t}$; these unitaries’ distribution in the thermodynamic limit is equal to that of Haar random unitaries (Theorem 2). Lastly, the linear map W from the space of t qubits to N_A qubits when $t \geq N_A$ can be written as a projected unitary, so that the distribution of states of the projected ensemble on A is equal to that of a projected Haar-random state on the dual chain. This can in turn be shown to be identical to that of a Haar-random state on A .

In this section, we discuss in a schematic fashion modifications of the above result and reasoning when we consider generalizations of the set-up: (i) for initial states describing a product state of spins uniformly pointing along an arbitrary direction in the x - y plane, and (ii) for the kicked Ising model with periodic boundary conditions.

A. Initial product state of spins uniformly lying in x - y plane

We consider a more general class of generator states from which the projected ensemble is derived from:

$$|\Psi(t)\rangle = U_F^t |\theta\rangle^{\otimes N}, \quad (\text{S6})$$

where $|\theta\rangle = e^{-i\theta S^z} |+\rangle$ describes a spin polarized along the $\cos \theta \hat{x} + \sin \theta \hat{y}$ direction. The case of $\theta = 0$ reduces to the scenario considered in the main text of the paper.

We expect the central result (Theorem 1 on the emergence of exact quantum state designs in the thermodynamic limit for $t \geq N_A$) should still hold for generic θ . Indeed, we can still employ our diagrammatic manipulations – leveraging the dual-unitary nature of the Floquet unitary to represent the projected state as arising from time-evolution in the dual-picture of t qubits initialized in $|+\rangle^{\otimes t}$ by a quantum circuit $\mathcal{U}(z_B)$, in which the measurement outcome z_B determines the particular quantum circuit applied. However, a difference from the case expounded in the main text is that the basic building blocks $U(z_{B,i}) \in \{U(0), U(1)\}$ that make up the circuit are more general: $U(z_{B,i})$ is identical in form and has parameters J, h, g similar to the Floquet unitary U_F (Eq. (4) of the main text), upon interpreting the site index i to run along the t -site dual chain, except with differing right boundary field $b_t = \pi/4(3\pi/4)$ that depends on the local measurement outcome $z_{B,i} = 0(1)$, and with left boundary field $b_1 = \pi/4 + \theta/2$. Consequently, we have to consider the statistics of this slightly more general (uniform) ensemble of unitaries $\{\mathcal{U}(z_B)\}$. One can repeat the proof of Theorem 2 (Sec. VII) almost verbatim, except with the modification that $g \mapsto g + \theta/2$ in Eq. (S46), to show that this ensemble of unitaries also forms an unitary design in the thermodynamic limit $N_B \rightarrow \infty$ for almost all θ (assuming $g \notin \mathbb{Z}\pi/8$).

B. Kicked Ising model with periodic boundary conditions

We consider next the kicked Ising model defined on a chain with periodic boundary conditions, that is, taking

$$H_{\text{Ising}} = J \sum_{i=1}^N \sigma_i^z \sigma_{i+1}^z + g \sum_{i=1}^N \sigma_i^z, \quad (\text{S7})$$

with $\sigma_{N+1}^\alpha = \sigma_1^\alpha$ ($\alpha = x, y, z$). As before, we fix $J = \pi/4$ and let g be arbitrary, excluding points $g \notin \mathbb{Z}\pi/8$. We focus on the generator state $|\Psi(t)\rangle = U_F^t |+\rangle^{\otimes t}$. Subsystem A here is taken to be any contiguous region of N_A qubits and B its complement.

Fig. S1a depicts the unnormalized projected state on A in the case with periodic boundary conditions. The Floquet unitary U_F still possesses a dual-unitary property, and so the same state can be written as shown in Fig. S1b. The diagram involves unitary evolution by the same depth- N_B quantum circuits $\mathcal{U}(z_B)$ as defined in the main text, except now summing over all states of the dual chain (thus effecting a trace). This is in contrast to the case with open boundary conditions, where the evolution is of only the particular initial state $|+\rangle^{\otimes t}$ on the dual chain. This difference is what prevents us from achieving an exact computation of the projected ensemble in the present model.

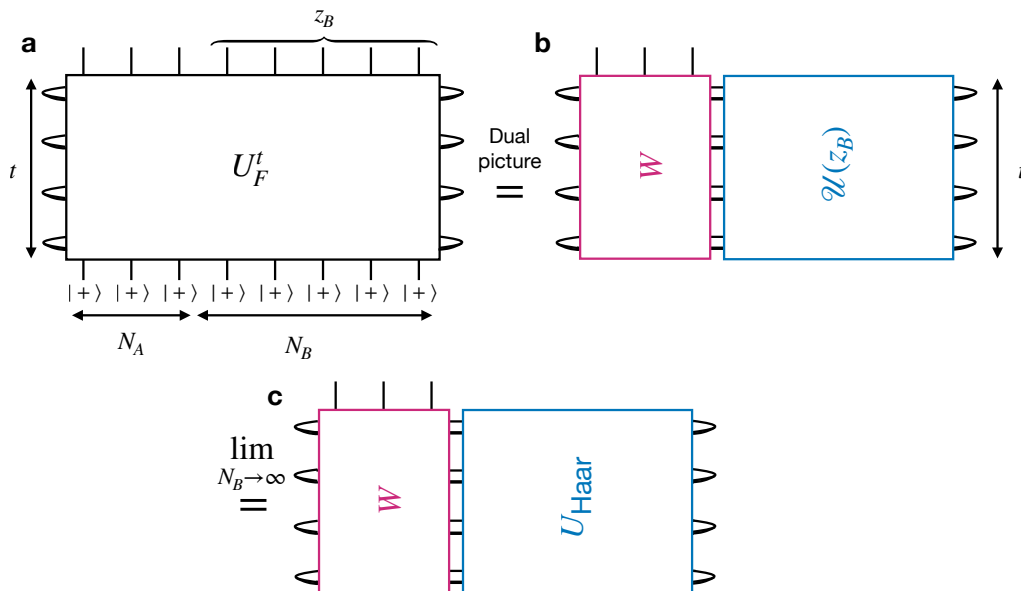


Figure S1. (a) Unnormalized projected state on A , obtained from time-evolution under the kicked Ising model defined with periodic boundary conditions (i.e. left and right boundaries are identified). (b) Using the dual-unitary nature of the Floquet unitary U_F , we can equivalently express the state as time-evolution of t qubits ('dual chain') by the quantum circuits $\mathcal{U}(z_B)$ (as defined in the main text). There is a sum over all initial configurations on the dual chain, effecting a trace. The linear map W , in contrast to that in the main text, now maps two copies of \mathbb{C}^{2^t} to $\mathbb{C}^{2^{N_A}}$. (c) In the TDL, the distribution of states of the projected ensemble \mathcal{E} is identical to a sum over all states on the dual chain (i.e. trace) evolved by Haar-random unitaries U_{Haar} , followed by the map W . All equalities are up to a multiplicative factor.

Note, the linear map W here, in contrast to that of the main text, maps states on *two* copies of \mathbb{C}^{2^t} to $\mathbb{C}^{2^{N_A}}$. Theorem 2 is still applicable though, which informs us that the distribution of $\mathcal{U}(z_B)$ in thermodynamic limit is identical to those of Haar random unitaries U_{Haar} , as shown in Fig. S1c.

What is the distribution of projected states as shown in Fig. S1c, as a function of time t ? To make progress, we employ numerics: we compute the quantum state ensemble pertaining to the random states as given by Fig. S1c, and compare their similarity to those of Haar randomly-generated states on A . More precisely, we consider the ensemble *estimate* \mathcal{E}_M comprised of M states where each corresponds to the evaluation of Fig. S1c, with each instance of the unitary U_{Haar} drawn independently from the Haar measure. We then compute the trace distance $\Delta^{(k)} = \frac{1}{2} \|\rho_{\mathcal{E}_M}^{(k)} - \rho_{\text{Haar}}^{(k)}\|_1$ of its moments to the corresponding moments of a Haar-random ensemble of states on A (S1). In the limit of $M \rightarrow \infty$ this will converge to the trace distance of the moments of the true projected ensemble, calculated in the thermodynamic limit, to those of Haar random states.

Fig. S2 shows the results for a subsystem A with $N_A = 2$ qubits and $g = \pi/9$. We see that for $k = 1$ and $t \geq 1$ the trace distance goes down indefinitely with sample size M , indicating that the trace distance of the actual projected ensemble, calculated in the thermodynamic limit, to Haar random states in fact vanishes. This observation is in perfect agreement with the analytic result of [4] proving that the entanglement entropy of a contiguous region of N_A qubits, computed for the kicked Ising model with periodic boundary conditions, is maximal once $t \geq \lceil N_A/2 \rceil$ (i.e. the reduced density matrix is maximally mixed). In contrast, for higher k s, it appears the trace distance converges at large enough M to a non-zero value for any fixed t , although the saturation value decreases with t . We are thus led to conjecture that the projected ensemble for the kicked Ising model with periodic boundary conditions, taking the thermodynamic limit first, only forms an approximate quantum state-design at any finite time t ; however, longer times makes this a better and better design. Note the difference from the case with open boundary conditions where there is instead a *finite* t beyond which the projected ensemble forms a provably-exact quantum state-design.

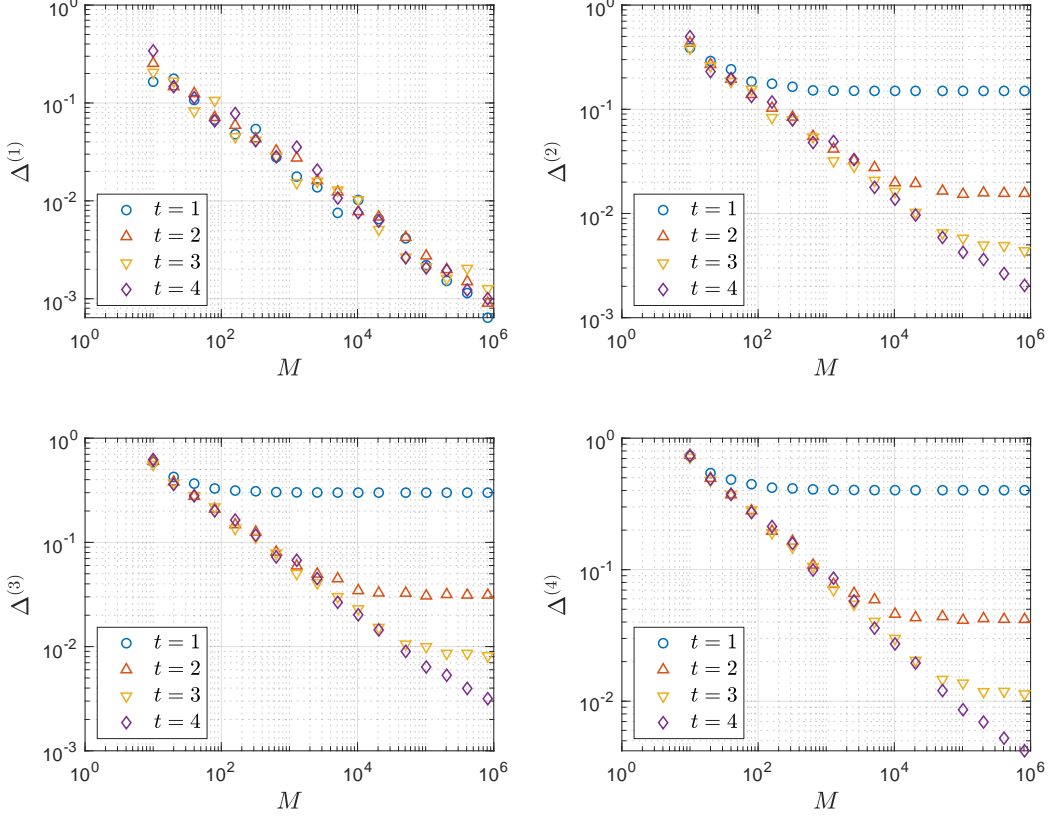


Figure S2. Trace distance $\Delta^{(k)}$ of the k -th moment of the quantum state ensemble formed by M samples of randomly generated states according to Fig. S1c, to the k -th moment of Haar randomly generated states. Here $N_A = 2$ and $g = \pi/9$.

III. DETAILS OF TENSOR NETWORK MANIPULATIONS

In this section we summarize some helpful properties of the basic diagrams used in the main text to represent U_F as a tensor-network. Recall we introduced the following elementary diagrams:

$$\text{---}\diamond\text{---} = \frac{1}{\sqrt{2}} \begin{pmatrix} 1 & 1 \\ 1 & -1 \end{pmatrix}, \quad \begin{array}{c} z_1 \\ \bullet \\ z_2 \end{array} \text{---} z_3 = \delta_{z_1 z_2 z_3} e^{-ig(1-2z_1)}. \quad (\text{S8})$$

Note a leg of either diagram carries two indices $z_i \in \{0, 1\}$; we have suppressed writing the indices in the former while explicitly written them in the latter. The former represents the standard Hadamard gate, while the latter is a three-legged tensor that evaluates to $e^{\mp ig}$ if $z_1 = z_2 = z_3 = 0(1)$ and 0 otherwise.

These tensors can be contracted, as is standard with tensor network manipulations, with one another or with quantum states (recall a contraction involves summing over all internal states). We note from the outset that all equalities presented below are to be understood as coming with the qualifier ‘‘up to global phases which are irrelevant’’. For example, the contraction of two three-legged tensors in the following manner yields a four-legged tensor:

$$\begin{array}{c} \diagup \bullet \diagdown \\ \diagdown \bullet \diagup \end{array} = \begin{array}{c} \bullet \\ \diagdown \diagup \\ \bullet \end{array} g_1 + g_2. \quad (\text{S9})$$

As can be verified, this diagram equals $e^{\mp i(g_1 + g_2)}$ if the indices of all four legs are 0(1), otherwise it equals 0. A contraction with the local state $|+\rangle = \frac{1}{\sqrt{2}}(|0\rangle + |1\rangle)$ yields, for example:

$$\begin{array}{c} \diagup \bullet \diagdown \\ \diagdown \bullet \diagup \end{array} |+\rangle = \frac{1}{\sqrt{2}} \times \begin{array}{c} \bullet \\ \diagdown \diagup \\ \bullet \end{array}. \quad (\text{S10})$$

This is nothing but a local gate proportional to a unitary effecting a z -rotation: $\frac{1}{\sqrt{2}} e^{-ig\sigma^z} = \frac{1}{\sqrt{2}} \begin{pmatrix} e^{-ig} & 0 \\ 0 & e^{ig} \end{pmatrix}$.

measurement outcome of (bulk) $N \times (t - 2)$ qubits of a 2D cluster state defined on a $N \times t$ rectangular grid, where the measurement is done in an appropriate local basis pointing in the XY-plane. Concretely, this is represented by the projection to the local state $\langle + | e^{-ig\sigma_z^\alpha}$ for each bulk qubit, such that the first ($\alpha = 1$) and last ($\alpha = t$) rows are not projected out. This connection between the 1D kicked Ising unitary and the 2D cluster state is ultimately what underlies the former's dual-unitary (more precisely, self-dual) nature.

V. DIAGRAMMATIC PROOF THAT W IS A PROJECTED UNITARY

In the main text we asserted that W , the linear map from the space of t qubits to N_A qubits (see Fig. 2b of the main text), is expressible for $t \geq N_A$ as

$$W = \sqrt{2}^{(t-N_A)} \langle + |^{\otimes (t-N_A)} V, \quad (\text{S16})$$

where V is a unitary on $\mathbb{C}^{2^{N_A}}$. That is, W is proportional to an isometry: $WW^\dagger \propto \mathbb{I}_{2^{N_A}}$. Fig. S3 illustrates this assertion. It involves repeated use of Eq. (S9).

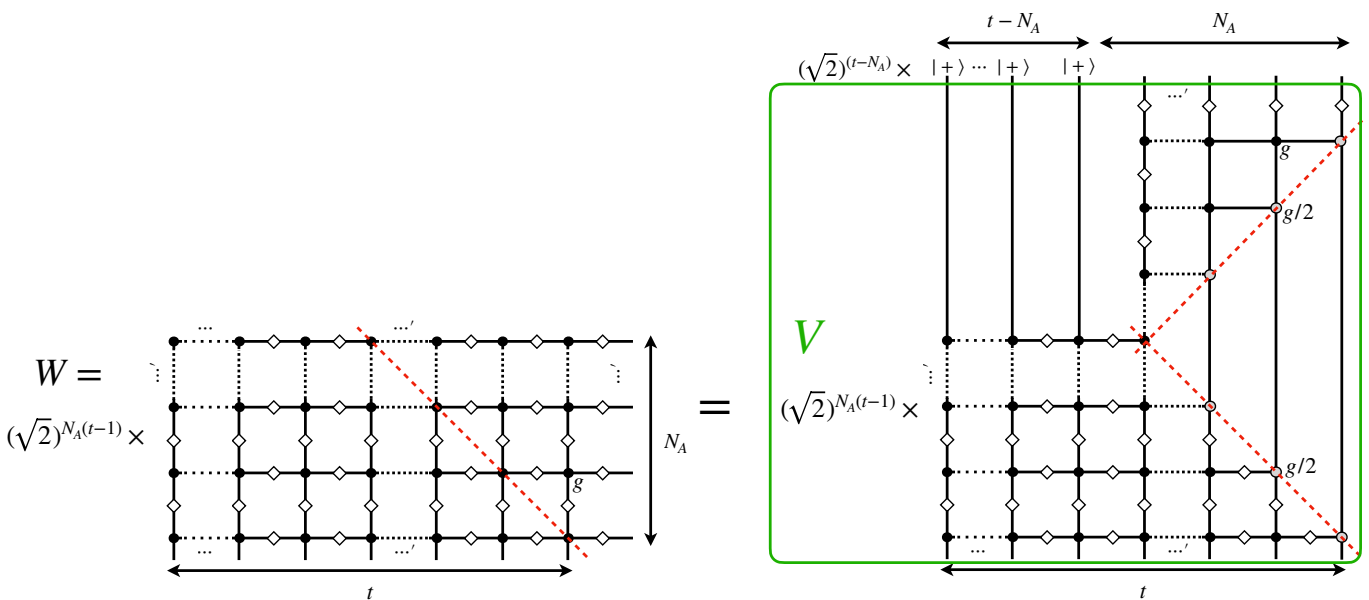


Figure S3. The linear map W (left) from the space of t qubits to N_A qubits, defined in Fig. 2b of the main text, can be expressed (right) for $t \geq N_A$ as $W = \sqrt{2}^{(t-N_A)} \langle + |^{\otimes (t-N_A)} V$, where V is a unitary on t qubits (green box). Note that \dots and \dots' represent different number of arbitrary qubits. To go from the left diagram to the right diagram, we have simply 'rotated' by 90° anti-clockwise the upper right part of the left diagram (above the dashed red diagonal line). Every black node carries the factor g , while nodes that live on the dashed red diagonal line get split into two grey nodes according to Eq. (S9), each of which carry the factor $g/2$.

VI. DETAILS OF THEOREM 1 (PROJECTED ENSEMBLE FORMS A QUANTUM STATE-DESIGN)

We justify more carefully the steps leading up to Theorem 1 of the main text. We start with the k -th moment of the projected ensemble represented in the dual picture as a (uniform) average of a function taking as input a depth- N_B quantum circuits $\mathcal{U}(z_B)$, with output $\frac{(\dots)^{\otimes k}}{(\dots)^{k-1}}$:

$$\rho_{\mathcal{E}}^{(k)} = \sum_{z_B} \frac{1}{2^{N_B}} \frac{(W\mathcal{U}(z_B)(|+\rangle\langle +|)^{\otimes t}\mathcal{U}(z_B)^\dagger W^\dagger)^{\otimes k}}{(\langle + |^{\otimes t}\mathcal{U}(z_B)^\dagger W^\dagger W\mathcal{U}(z_B)|+\rangle^{\otimes t})^{k-1}}. \quad (\text{S17})$$

Theorem 2 states that the (uniform) ensemble of unitaries $\{\mathcal{U}(z_B)\}$ forms an exact unitary designs in the thermo-

dynamic limit. Therefore, taking the TDL, $\rho_{\mathcal{E}}^{(k)}$ can be expressed

$$\begin{aligned}
\lim_{N_B \rightarrow \infty} \rho_{\mathcal{E}}^{(k)} &= \lim_{N_B \rightarrow \infty} \sum_{z_B} \frac{2^{(t-N_A)} \left(\langle + |^{\otimes(t-N_A)} V \mathcal{U}(z_B) (|+\rangle \langle +|)^{\otimes t} \mathcal{U}(z_B)^\dagger V^\dagger |+\rangle^{\otimes(t-N_A)} \right)^{\otimes k}}{2^{N_B} \left(\langle + |^{\otimes t} \mathcal{U}(z_B)^\dagger V^\dagger (|+\rangle \langle +|)^{\otimes(t-N_A)} V \mathcal{U}(z_B) |+\rangle^{\otimes t} \right)^{k-1}} \\
&= \int_{U \sim \text{Haar}(2^t)} dU 2^{(t-N_A)} \frac{\left(\langle + |^{\otimes(t-N_A)} V U (|+\rangle \langle +|)^{\otimes t} U^\dagger V^\dagger |+\rangle^{\otimes(t-N_A)} \right)^{\otimes k}}{\left(\langle + |^{\otimes t} U^\dagger V^\dagger (|+\rangle \langle +|)^{\otimes(t-N_A)} V U |+\rangle^{\otimes t} \right)^{k-1}} \\
&= \int_{U \sim \text{Haar}(2^t)} dU 2^{(t-N_A)} \frac{\left(\langle + |^{\otimes(t-N_A)} U (|+\rangle \langle +|)^{\otimes t} U^\dagger |+\rangle^{\otimes(t-N_A)} \right)^{\otimes k}}{\left(\langle + |^{\otimes t} U^\dagger (|+\rangle \langle +|)^{\otimes(t-N_A)} U |+\rangle^{\otimes t} \right)^{k-1}} \\
&= \int_{\Psi \sim \text{Haar}(2^t)} d\Psi 2^{(t-N_A)} \frac{|\Psi_+\rangle \langle \Psi_+|^{\otimes k}}{\langle \Psi_+ | \Psi_+ \rangle^{k-1}}, \\
&= \int_{\Psi \sim \text{Haar}(2^t)} d\Psi \frac{(|\Psi_+\rangle \langle \Psi_+|)^{\otimes k}}{\langle \Psi_+ | \Psi_+ \rangle^k} \times 2^{t-N_A} \langle \Psi_+ | \Psi_+ \rangle
\end{aligned} \tag{S18}$$

where $|\Psi_+\rangle := \langle + |^{\otimes(t-N_A)} |\Psi\rangle$.

The first equality uses the form of W , (S16). To justify the second equality, we express the denominator of (S17) as a power series: $\frac{1}{x^{k-1}} = \frac{1}{1-(1-x^{k-1})} = \sum_{\alpha=0}^{\infty} (1-x^{k-1})^\alpha$, where $x = \langle + |^{\otimes t} \mathcal{U}(z_B)^\dagger V^\dagger (|+\rangle \langle +|)^{\otimes(t-N_A)} V \mathcal{U}(z_B) |+\rangle^{\otimes t} \in [0, 1]$.

Note the $x = 0$ case (vanishing projected state) is excluded in the definition of $\rho_{\mathcal{E}}^{(k)}$. This power series, which has a radius of convergence $|1 - x^{k-1}| < 1$, thus converges absolutely for the values of x we are interested in. We can hence distribute the sum over z_B over each power of α in the expansion and take the TDL $N_B \rightarrow \infty$ (this step is justified from Tonelli's or Fubini's theorem); together with the numerator, each term is a polynomial in U, U^\dagger of finite degree (equal powers for both) for which we can apply Theorem 2, converting the sum into an integral over unitaries drawn from the Haar measure. Then we can reverse the process and resum the terms to yield the second line of Eq. (S18). The third equality arises from the invariance of the Haar measure which we use to absorb the unitary V . The fourth equality uses that the state $|\Psi\rangle = U|+\rangle^{\otimes t}$ is Haar-random distributed should the unitary U be Haar-random distributed. It expresses that the resulting quantity is the expected k -th moment of the projected ensemble formed from Haar random states $|\Psi\rangle \in (\mathbb{C}^2)^{\otimes t}$, where $t - N_A$ sites are projected out. The fifth equality is a rewriting of the fourth line.

Now, Lemma 4 of Ref. [6] states that the random variables $(|\Psi_+\rangle \langle \Psi_+|)^{\otimes k} / \langle \Psi_+ | \Psi_+ \rangle^k$ and $2^{t-N_A} \langle \Psi_+ | \Psi_+ \rangle$ are independent. We reproduce the argument here. We shift $|\Psi\rangle \mapsto U_A |\Psi\rangle$ for some fixed unitary U_A supported only on A ; the resulting state is still Haar-randomly distributed over the full Hilbert space. However we note that $2^{t-N_A} \langle \Psi_+ | \Psi_+ \rangle$ is invariant under this transformation while $(|\Psi_+\rangle \langle \Psi_+|)^{\otimes k} / \langle \Psi_+ | \Psi_+ \rangle^k \mapsto (U_A |\Psi_+\rangle \langle \Psi_+| U_A^\dagger)^{\otimes k} / \langle \Psi_+ | \Psi_+ \rangle^k$. Now if we average over U_A assuming it is uniformly generated, the latter is nothing more than k -th moment $\rho_{\text{Haar}}^{(k)}$ of the Haar random ensemble of states on $\mathbb{C}^{2^{N_A}}$, (S1). Explicitly,

$$\begin{aligned}
&\int_{\Psi \sim \text{Haar}(2^t)} d\Psi \frac{(|\Psi_+\rangle \langle \Psi_+|)^{\otimes k}}{\langle \Psi_+ | \Psi_+ \rangle^k} 2^{t-N_A} \langle \Psi_+ | \Psi_+ \rangle \\
&= \int_{\Psi \sim \text{Haar}(2^t)} d\Psi \frac{(U_A |\Psi_+\rangle \langle \Psi_+| U_A^\dagger)^{\otimes k}}{\langle \Psi_+ | \Psi_+ \rangle^k} 2^{t-N_A} \langle \Psi_+ | \Psi_+ \rangle \text{ (some fixed } U_A) \\
&= \int_{\Psi \sim \text{Haar}(2^t)} d\Psi \int_{U_A \sim \text{Haar}(2^{N_A})} dU_A \frac{(U_A |\Psi_+\rangle \langle \Psi_+| U_A^\dagger)^{\otimes k}}{\langle \Psi_+ | \Psi_+ \rangle^k} 2^{t-N_A} \langle \Psi_+ | \Psi_+ \rangle \text{ (uniformly averaging over } U_A) \\
&= \int_{\Psi \sim \text{Haar}(2^t)} d\Psi \int_{\psi \sim \text{Haar}(2^{N_A})} d\psi (|\psi\rangle \langle \psi|)^{\otimes k} \times 2^{t-N_A} \langle \Psi_+ | \Psi_+ \rangle \\
&= \int_{\psi \sim \text{Haar}(2^{N_A})} d\psi (|\psi\rangle \langle \psi|)^{\otimes k} \times \int_{\Psi \sim \text{Haar}(2^t)} d\Psi 2^{t-N_A} \langle \Psi_+ | \Psi_+ \rangle \\
&= \rho_{\text{Haar}}^{(k)} \times 1.
\end{aligned} \tag{S19}$$

VII. PROOF OF THEOREM 2 (\mathcal{E}_U FORMS A UNITARY DESIGN)

Here we prove that the distribution of unitaries $\mathcal{U}(z_B)$ which act on t qubits, formed from all possible length- N_B products of $U(0), U(1)$ specified by the bit-string z_B , each occurring with equal probability, becomes uniformly

distributed over the unitary group in the thermodynamic limit:

Theorem 2. For $g \notin \mathbb{Z}\pi/8$, the unitary ensemble \mathcal{E}_U forms an exact unitary-design in the TDL. That is, all moments k of \mathcal{E}_U and the Haar-random unitary ensemble agree:

$$\lim_{N_B \rightarrow \infty} \sum_{z_B} \frac{1}{2^{N_B}} \mathcal{U}(z_B)^{\otimes k} \otimes \mathcal{U}(z_B)^{* \otimes k} = \int_{U \sim \text{Haar}(2^t)} dU U^{\otimes k} \otimes U^{* \otimes k} \quad (\text{S20})$$

where $(\cdot)^*$ denotes complex conjugation.

Proof. Instead of working with Eq. (S20), which is one definition of a *unitary k -ensemble*, we use an equivalent definition: for any operator X on $(\mathbb{C}^{2^t})^{\otimes k}$,

$$\lim_{N_B \rightarrow \infty} \mathcal{T}_{\mathcal{E}_U}^{(k)}[X] = \mathcal{T}_{\text{Haar}}^{(k)}[X], \quad (\text{S21})$$

where $\mathcal{T}_{\mathcal{E}_U}^{(k)}[X] := \frac{1}{2^{N_B}} \sum_{z_B} \mathcal{U}(z_B)^{\otimes k} X \mathcal{U}(z_B)^{\dagger \otimes k}$ and $\mathcal{T}_{\text{Haar}}^{(k)}[X] := \int_{U \sim \text{Haar}(2^t)} dU U^{\otimes k} X U^{\dagger \otimes k}$ are so-called *k -fold twirls* over the respective unitary ensembles [3].

Our strategy is to show that the action of $\mathcal{T}_{\mathcal{E}_U}^{(k)}$ and $\mathcal{T}_{\text{Haar}}^{(k)}$ agree in the thermodynamic limit. To begin, we observe we can express the k -fold twirl over the projected ensemble $\mathcal{T}_{\mathcal{E}}^{(k)}$ as a transfer map $\mathbb{T}^{(k)}$ raised to the N_B -th power:

$$\begin{aligned} \mathcal{T}_{\mathcal{E}_U}^{(k)}[X] &= \frac{1}{2^{N_B}} \sum_{z_B \in \{0,1\}^{N_B}} \mathcal{U}(z_B)^{\otimes k} X \mathcal{U}(z_B)^{\dagger \otimes k} \\ &= \sum_{z_B \in \{0,1\}^{N_B}} \frac{1}{2^{N_B}} \prod_{i=1}^{N_B} U(z_{B,i})^{\otimes k} X \prod_{i=1}^{N_B} U(z_{B,i})^{\dagger \otimes k} \\ &= \left(\frac{1}{2} \sum_{z_{B,1} \in \{0,1\}} U(z_{B,1})^{\otimes k} \left(\frac{1}{2} \sum_{z_{B,2} \in \{0,1\}} U(z_{B,2})^{\otimes k} \dots \left(\frac{1}{2} \sum_{z_{B,N_B} \in \{0,1\}} U(z_{B,N_B})^{\otimes k} X U(z_{B,N_B})^{\dagger \otimes k} \right) \dots U(z_{B,2})^{\dagger \otimes k} \right) U(z_{B,1})^{\dagger \otimes k} \right) \\ &= (\mathbb{U}^{(k)} \circ \mathbb{P}^{(k)})^{N_B}[X] \\ &= (\mathbb{T}^{(k)})^{N_B}[X]. \end{aligned} \quad (\text{S22})$$

In the second line, we used the definition of $\mathcal{U}(z_B)$ as a product of unitaries $\mathcal{U}(z_B) = \prod_{i=1}^{N_B} U(z_{B,i})$, ordered so that the index $i = N_B(1)$ appears left(right)-most. In the third line, we exchanged the sum and product. In the fourth line, we defined linear maps $\mathbb{U}^{(k)}, \mathbb{P}^{(k)}$ which act on operators on $(\mathbb{C}^{2^t})^{\otimes k}$

$$\begin{aligned} \mathbb{U}^{(k)}[X] &:= U(0)^{\otimes k} X U(0)^{\dagger \otimes k}, \\ \mathbb{P}^{(k)}[X] &:= \frac{1}{2} (X + (\sigma_t^z)^{\otimes k} X (\sigma_t^z)^{\otimes k}). \end{aligned} \quad (\text{S23})$$

Here $U(0)$ is identical to the Ising unitary U_F , Eq. (4) of the main text, interpreted to act on a spin chain of t qubits (the ‘dual chain’). In the fifth line, we defined the transfer map $\mathbb{T}^{(k)}$ as the composition of the linear map $\mathbb{U}^{(k)}$ and $\mathbb{P}^{(k)}$.

Since $\mathbb{U}^{(k)}$ is a conjugation by unitaries, it is a norm-preserving map, while since $\mathbb{P}^{(k)}$ is a projection $(\mathbb{P}^{(k)})^2 = \mathbb{P}^{(k)}$, it has eigenvalues 0, 1. This immediately leads to the following two properties of $\mathbb{T}^{(k)}$: (i) its eigenvalues λ have at most unit magnitude, (ii) the algebraic and geometric multiplicities of unimodular eigenvalues $|\lambda| = 1$ coincide, even if $\mathbb{T}^{(k)}$ is not diagonalizable. These properties are identical to those of the transfer matrix used in [7] to compute the spectral form factor of the kicked Ising model, owing to a similar form (there it was the composition of a unitary and a map with at most unit eigenvalues). We refer the reader to [7] for the proof of these properties, which carry over *mutatis mutandis*.

For any finite t and k , any non-unimodular eigenvalues of the linear map $\mathbb{T}^{(k)}$ will be separated from the unimodular ones by a finite gap $\Delta_{\text{gap}} = 1 - \max_{\lambda: |\lambda| < 1} |\lambda|$, and have magnitude less than unity. Hence, they will vanish when raised to an infinitely-high power $N_B \rightarrow \infty$ (the thermodynamic limit). To understand the action of $(\mathbb{T}^{(k)})^{N_B}$ in the TDL, we therefore need only find the unimodular eigenvalues of $\mathbb{T}^{(k)}$ and their eigenoperators X , which satisfy

$$\mathbb{T}^{(k)}[X] = e^{i\theta} X. \quad (\text{S24})$$

Expanding X (which is assumed without loss of generality normalized) in terms of orthonormal eigenoperators X_0 and X_1 of \mathbb{P} with eigenvalues 0, 1 respectively, we have $X = c_0 X_0 + c_1 X_1$ (the inner product is under the Hilbert-Schmidt or Frobenius inner product) with $|c_0|^2 + |c_1|^2 = 1$. Now since

$$1 = \text{Tr}(X^\dagger X) = \text{Tr}\left(\mathbb{T}^{(k)}[X]^\dagger \mathbb{T}^{(k)}[X]\right) = \text{Tr}\left(\mathbb{P}^{(k)}[X]^\dagger \mathbb{P}^{(k)}[X]\right) = |c_1|^2 \text{Tr}\left(X_1^\dagger X_1\right) = |c_1|^2, \quad (\text{S25})$$

this is possible if and only if $c_0 = 0$. Therefore, our desired X further satisfy the conditions

$$\mathbb{P}^{(k)}[X] = X, \quad \mathbb{U}^{(k)}[X] = e^{i\theta} X, \quad (\text{S26})$$

which can be rewritten straightforwardly, using the definition of the maps (S23), as

$$[(\sigma_t^z)^{\otimes k}, X] = 0, \quad U(0)^{\otimes k} X U(0)^{\dagger \otimes k} = e^{i\theta} X. \quad (\text{S27})$$

Now consider the family of unitary operators on \mathbb{C}^{2^t}

$$V_p := U(0)^p \sigma_t^z U(0)^{-p}, \quad p \in \mathbb{Z}. \quad (\text{S28})$$

Note $\sigma_t^z \propto U(0)^{-1} U(1)$ so V_p can in fact be written as some product of $U(0)$, $U(1)$ and their inverses. From Eq. (S27), it is immediate that X must also satisfy that it commutes with any (unitary) element of the set comprised of a product of $V_{p_i}^{\otimes k}$:

$$[V_{p_1}^{\otimes k} V_{p_2}^{\otimes k} V_{p_3}^{\otimes k} \dots, X] = 0. \quad (\text{S29})$$

By continuity of the k -th tensor power and commutator, X also commutes with all limit points of this set.

Lemma 1 below specifies that for $g \notin \mathbb{Z}\pi/8$, one can construct single-site rotations as well as entangling nearest-neighbor two-site unitary gates on \mathbb{C}^{2^t} from products of V_p . As is well known from the theory of quantum computation [8], such a set is *universal*, in the sense that the set of unitaries generated from it is dense in the space of all unitary operators V acting on the Hilbert space \mathbb{C}^{2^t} . Therefore, again by continuity, and completeness of the space of unitaries, eigenoperators X of $\mathbb{T}^{(k)}$ with unimodular eigenvalues for such g satisfy for any unitary V on \mathbb{C}^{2^t} ,

$$[V^{\otimes k}, X] = 0 \iff \int_{V \sim \text{Haar}(2^t)} dV V^{\otimes k} X V^{\dagger \otimes k} = X. \quad (\text{S30})$$

We note that the right hand side is nothing but the condition for eigenoperators of $\mathcal{T}_{\text{Haar}}^{(k)}$ with eigenvalue +1. From the Schur-Weyl duality, we know that all solutions to Eq. (S30) are given by linear combination of permutation operators $P(\pi)$,

$$X = \sum_{\pi \in S^k} c_\pi P(\pi), \quad (\text{S31})$$

where $P(\pi)$ acts on $(\mathbb{C}^{2^t})^{\otimes k}$ and permutes the k copies of the Hilbert space \mathbb{C}^{2^t} according to a member π of the permutation group S_k on k elements:

$$P(\pi)|i_1, i_2, \dots, i_k\rangle = |i_{\pi(1)}, i_{\pi(2)}, \dots, i_{\pi(k)}\rangle, \quad 1 \leq i \leq 2^t. \quad (\text{S32})$$

Note that the permutation operators $P(\pi)$ are not orthonormal: $\text{Tr}(P(\pi)^\dagger P(\pi')) \propto \delta_{\pi, \pi'}$. Indeed, while the number of elements π of S_k is $k!$, the dimension of the vector space spanned by $P(\pi)$ is only $k!$ if the dimension is large enough, namely when $2^t \geq k$.

The solution Eq. (S31) is ‘universal’ [9], and entails that $\theta = 0$ in Eq. (S27). Thus, we see that for $g \notin \mathbb{Z}\pi/8$, all unimodular eigenoperators of $\mathcal{T}_{\mathcal{E}_U}^{(k)}$ have eigenvalues +1 and that their span coincides with the +1 eigenspace of $\mathbb{T}_{\text{Haar}}^{(k)}$. Since states in the subspace orthogonal to the +1 eigenspace of $\mathbb{T}_{\text{Haar}}^{(k)}$ carry 0 eigenvalue under $\mathbb{T}_{\text{Haar}}^{(k)}$ (owing to it being a projector), and also map to the zero vector under $\lim_{N_B \rightarrow \infty} \mathbb{T}_{\mathcal{E}_U}^{(k)}$, we therefore have that the actions of $\lim_{N_B \rightarrow \infty} \mathcal{T}_{\mathcal{E}_U}^{(k)}$ and $\mathcal{T}_{\text{Haar}}^{(k)}$ match. This concludes the proof. \blacksquare

VIII. NUMERICAL VERIFICATION AND GAP OF TRANSFER MATRIX

We check the necessity of the condition $g \notin \mathbb{Z}\pi/8$ required of Theorem 2. Numerically, we find that $g = (2m + 1)\pi/8, m \in \mathbb{Z}$ also yields unitary-designs while $g = m\pi/4, m \in \mathbb{Z}$ do not, see Fig. S4 where we plot the gap $\Delta = 1 - |\lambda_{k!+1}|$ of the transfer matrix $\mathbb{T}^{(k)}$ separating the $k!$ ‘universal’ unimodular eigenoperators (S31) from the ‘non-universal’ non-unimodular ones (we ensured the Hilbert space dimension is large enough, $2^t \geq k$). Note a finite gap implies the formation of unitary-designs in the TDL, which we see from Fig. S4 occurs everywhere except $g \in \mathbb{Z}\pi/4$. This implies $g \notin \mathbb{Z}\pi/8$ is only a sufficient (but not necessary) condition for \mathcal{E}_U to form a unitary-design, and suggests that the proof of Theorem 2 can be further improved. Note that the definition of gap here differs from that in the preceding section, though they coincide for parameters g away from $\mathbb{Z}\pi/4$. At those points, there are additional (non-universal) eigenoperators with unimodular eigenvalues of $\mathbb{T}^{(k)}$ than just given by Eq. (S31).

Intuitively, the gap Δ computed here sets the rate of convergence with N_B of the unitary ensemble \mathcal{E}_U to form a unitary k -design, and correspondingly, the rate of convergence of the state ensemble \mathcal{E} to a quantum state k -design. Establishing this connection more precisely would be an extremely interesting direction for future investigation.

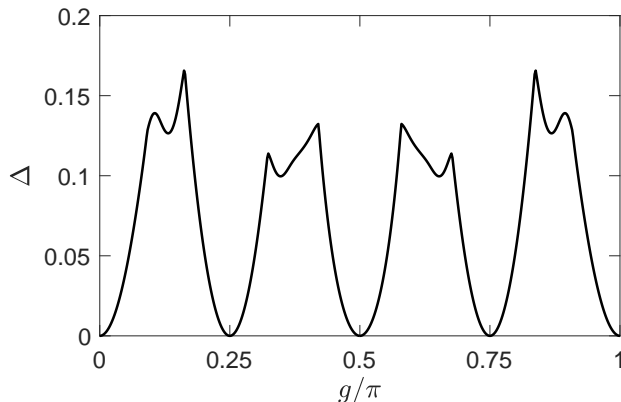


Figure S4. Gap $\Delta = 1 - |\lambda_{k!+1}|$ of transfer matrix $\mathbb{T}^{(k)}$ for $t = 3$ and $k = 2$. Note the number of unit eigenvalues $\lambda = +1$ is equal to 2 for $g \notin \mathbb{Z}\pi/4$. One sees that the transfer matrix is gapped except for $g = \mathbb{Z}\pi/4$ – indeed, we find numerically that the projected ensemble \mathcal{E} does not (does) form a quantum state-design in the thermodynamic limit at (away from) those points.

IX. PROOF OF LEMMAS

A. Lemma 1 (Construction of universal gate set)

In Theorem 2, we utilized the following Lemma:

Lemma 1. *Let $g \notin \mathbb{Z}\pi/8$. Consider the set \mathcal{S} of unitaries acting on \mathbb{C}^{2^t} generated from products of V_p , as well as its limit points. Then this set contains arbitrary single-site rotations and nearest-neighbor two-site entangling gates, which forms a universal gate set on \mathbb{C}^{2^t} .*

Proof. Let us first recall the definition of V_p :

$$V_p := U(0)^p \sigma_i^z U(0)^{-p}, \quad p \in \mathbb{Z}, \quad (\text{S33})$$

where $U(0)$ is identical to (S4), but interpreted to act on a 1D chain of t qubits (dual chain). Because of the choice of parameters, up to an irrelevant global phase, $U(0)$ can equivalently be written as

$$U(0) = \left(\prod_{i=1}^t H_i \right) \left(e^{-ig \sum_{i=1}^t \sigma_i^z} \right) \left(\prod_{i=1}^{t-1} \text{CZ}_{i,i+1} \right) \quad (\text{S34})$$

where $\text{CZ}_{i,j}$ is the control- Z gate acting on a pair of qubits (i, j) , and H_i is the Hadamard gate acting on site i :

$$\text{CZ}_{i,j} = \begin{pmatrix} 1 & & & \\ & 1 & & \\ & & 1 & \\ & & & -1 \end{pmatrix}_{i,j}, \quad H_i = \frac{1}{\sqrt{2}} \begin{pmatrix} 1 & 1 \\ 1 & -1 \end{pmatrix}_i. \quad (\text{S35})$$

This can be immediately read off from the tensor network diagram, Fig. 2 of the main text.

We now prove Lemma 1 via induction. We first focus on single-site rotations: the proposition $P(i)$ for $2 \leq i \leq t$ is that the operators

$$\begin{aligned} & \sigma_{i-1}^x e^{-ig\sigma_i^x} \sigma_i^z e^{ig\sigma_i^x}, \\ & \sigma_{i-1}^z e^{ig\sigma_i^z} \sigma_i^x e^{-ig\sigma_i^z}, \end{aligned} \quad (\text{S36})$$

along with arbitrary single-qubit rotations on site i , are in the set \mathcal{S} .

We first show this for $i = t$. We evaluate V_{-1}, V_0, V_1, V_2 , using (S33), (S34):

$$V_{-1} = \sigma_{t-1}^z e^{ig\sigma_t^z} \sigma_t^x e^{-ig\sigma_t^z} \quad (\text{S37})$$

$$V_0 = \sigma_t^z, \quad (\text{S38})$$

$$V_1 = \sigma_t^x, \quad (\text{S39})$$

$$V_2 = \sigma_{t-1}^x e^{-ig\sigma_t^x} \sigma_t^z e^{ig\sigma_t^x}. \quad (\text{S40})$$

The following products, which are single-qubit rotations acting non-trivially only on site t , are also in \mathcal{S} :

$$\begin{aligned} W_1 &= V_{-1} V_1 V_2 V_0 V_{-1} V_1 V_2 V_0 = e^{i2g\sigma_t^z} e^{-i2g\sigma_t^x} e^{i2g\sigma_t^z} e^{-i2g\sigma_t^x}, \\ W_2 &= V_{-1} V_1 V_{-1} V_1 = e^{i4g\sigma_t^z}. \end{aligned} \quad (\text{S41})$$

Parametrizing these rotations by $W_i = e^{-i\theta_i \hat{n}_i \cdot \vec{S}}$ where θ is the rotation angle and \hat{n} is the unit vector specifying the axis of rotation, with $\vec{S} = (\sigma^x, \sigma^y, \sigma^z)/2$, we have

$$\begin{aligned} \theta_1 &= 2 \arccos(2 \cos^4(2g) - 1), \\ \hat{n}_1 &= \frac{(2 \cos^3(2g) \sin(2g), -\sin^2(4g)/2, -2 \cos^3(2g) \sin(2g))}{\sqrt{1 - (-1 + 4 \cos(4g) + \cos(8g))^2/16}}, \\ \theta_2 &= -8g, \\ \hat{n}_2 &= (0, 0, 1). \end{aligned} \quad (\text{S42})$$

We now consider the conditions on g sufficient for products of W_1, W_2 to generate densely all rotations on the Bloch sphere. What is well known is if the angle between the rotation axes is between 0 and $\pi/2$, and that at least one of the rotation angles is an irrational multiple of π and the other is not a trivial rotation, i.e. a multiple of 2π , this will occur. From (S42) we see that as long as $g \notin \mathbb{Z}\pi/4$, the angle between the rotation axes \hat{n}_1 and \hat{n}_2 is between 0 and $\pi/2$. Next let us first assume θ_2 is an irrational multiple of π . Then it suffices to impose similarly $g \notin \mathbb{Z}\pi/4$ to avoid θ_1 being a multiple of 2π . Now let us assume θ_2 (or equivalently, g) is a rational multiple of π . Lemma 2 shows that θ_1 is an irrational multiple of π if and only if $g \notin \mathbb{Z}\pi/8$. Therefore, $g \notin \mathbb{Z}\pi/8$ is a sufficient condition to ensure that the rotations W_1, W_2 generate densely any single-site rotation on site t , and so \mathcal{S} contains *arbitrary* single-site rotations on site t .

Now we show the implication $P(i) \implies P(i-1)$. From (S36) and the presence of arbitrary single-site rotations on site i we have that unitaries

$$\sigma_{i-1}^z, \sigma_{i-1}^x, \quad (\text{S43})$$

as well as

$$\sigma_{i-1}^x \sigma_i^z, \sigma_{i-1}^z \sigma_i^x \quad (\text{S44})$$

are in \mathcal{S} . Hence so are

$$\begin{aligned} U(0) \sigma_{i-1}^x \sigma_i^z U(0)^{-1} &= \sigma_{i-2}^x e^{-ig\sigma_{i-1}^x} \sigma_{i-1}^z e^{ig\sigma_{i-1}^x}, \\ U(0)^{-1} \sigma_{i-1}^z \sigma_i^x U(0) &= \sigma_{i-2}^z e^{ig\sigma_{i-1}^z} \sigma_{i-1}^x e^{-ig\sigma_{i-1}^z}, \end{aligned} \quad (\text{S45})$$

(this requires $i \geq 2$), as they can both be expressed as a limiting sequence of products of V_p s. Note the operators contained in (S43), (S45) are identical to V_{-1}, V_0, V_1, V_2 , ignoring the site index. Therefore we can similarly construct W_1, W_2 as above (dropping the site-index), repeat the same argument *mutatis mutandis*, to find that arbitrary single-site rotations on site $i-1$ are in the set \mathcal{S} . Thus, we recover proposition $P(i-1)$.

Lastly we consider the case of site $i = 1$. Proposition $P(2)$ implies the operators $\sigma_1^x \sigma_2^z, \sigma_1^z \sigma_2^x$ are in \mathcal{S} . Conjugating by $U(0)$ and its inverse gives

$$\begin{aligned} U(0)\sigma_1^x\sigma_2^zU(0)^{-1} &= e^{-ig\sigma_1^x}\sigma_1^z e^{ig\sigma_1^x}, \\ U(0)^{-1}\sigma_1^z\sigma_2^xU(0) &= e^{ig\sigma_1^z}\sigma_1^x e^{-ig\sigma_1^z}. \end{aligned} \quad (\text{S46})$$

Products of these two unitaries assuming $g \notin \mathbb{Z}\pi/8$ generate densely all single-qubit unitaries on site $i = 1$. Therefore one-half of lemma 1 is proved, namely that \mathcal{S} contains all single-site rotations.

For the second-half of lemma 1, let $Q(j)$, $2 \leq j \leq t$, be the proposition that the two-site entangling gates

$$E_{j-1,j} := U(0) \prod_{i=j+1}^t \text{CZ}_{i-1,i} H_j \prod_{i=j+1}^t \text{CZ}_{i-1,i} U(0)^{-1} \quad (\text{S47})$$

are in \mathcal{S} . Note $E_{j-1,j}$ can be evaluated straightforwardly from the definition of $U(0)$ (S34) to be

$$E_{j-1,j} = \left(H_{j-1} H_j e^{-ig(\sigma_{j-1}^z + \sigma_j^z)} \right) \times \text{CZ}_{j-1,j} H_j \text{CZ}_{j-1,j} \times \left(e^{ig(\sigma_{j-1}^z + \sigma_j^z)} H_j H_{j-1} \right). \quad (\text{S48})$$

To see that it is entangling, it suffices to show its action on a particular product state yields an entangled state. We evaluate its action (restricting it to be on sites $j-1, j$ for notational simplicity) on the product state $|\chi\rangle_{j-1,j} := e^{-ig(\sigma_{j-1}^z + \sigma_j^z)} H_{j-1} H_j |+\rangle_{j-1} |+\rangle_j$:

$$E_{j-1,j} |\chi\rangle_{j-1,j} = H_{j-1} H_j e^{-ig(\sigma_{j-1}^z + \sigma_j^z)} (|0\rangle_{j-1} |0\rangle_j - |1\rangle_{j-1} |1\rangle_j), \quad (\text{S49})$$

which is maximally entangled.

Now we prove the propositions $Q(j)$. Obviously $Q(t)$ is true since $E_{t-1,t} = U(0)H_tU(0)^{-1}$ is in \mathcal{S} , as H_t is a single-site rotation. Next we prove that $Q(j), Q(j+1), \dots, Q(t) \implies Q(j-1)$. As $E_{j-1,j}, E_{j,j+1}, \dots, E_{t-1,t}$ are entangling gates, they, together with arbitrary single site rotations on sites $j-1, j, \dots, t$, form a universal gate set on qubits $j-1, j, \dots, t$, a well-known fact in the theory of quantum computation [8]. That is, we can construct from them arbitrary *global* rotations on these qubits. In particular, we can construct the unitary $\text{CZ}_{j-1,j} \text{CZ}_{j,j+1} \dots \text{CZ}_{t-1,t} H_j \text{CZ}_{t-1,t} \dots \text{CZ}_{j,j+1} \text{CZ}_{j-1,j}$, and hence it follows that $E_{j-2,j-1}$ is in set \mathcal{S} .

Combing the two parts, we therefore have that \mathcal{S} contains arbitrary single-site rotations and nearest-neighbor two-site entangling gates, which constitutes a universal gate set on \mathbb{C}^{2^t} . \blacksquare

B. Lemma 2 (Irrationality of θ_1)

Lemma 2. *Let g be a rational angle, that is, $g = \frac{p}{q}\pi$ for some $p, q \in \mathbb{Z}$, $q \geq 1$. Then $\theta_1/\pi = \frac{1}{\pi} 2 \arccos(2 \cos^4(2g) - 1)$ is irrational if and only if g is not divisible by $\pi/8$.*

Proof. The ‘‘only if’’ direction is straightforward: suppose by contradiction there exists some g divisible by $\pi/8$ such that θ_1/π is irrational. From $\theta_1 = 2 \arccos(2 \cos^4(2g) - 1)$ we see that we need only consider $g \in [0, \pi/2]$, so we just have to check the cases $g = 0, \pi/8, \pi/4, 3\pi/4, \pi/2$. This yields $\theta_1/\pi = 0, 4/3, 2, 4/3, 0$ respectively, which are all rational. Thus, θ_1/π not rational implies g not divisible by $\pi/8$.

The ‘‘if’’ direction is difficult [10]. Suppose by contradiction there exists some g not divisible by $\pi/8$ such that θ_1/π is rational. Then $\theta_1 = 4h$ for some h which is a rational multiple of π . This implies $2 \cos^4(2g) - 1 = \cos(2h)$ which further implies $2 \cos^4(2g) = 2 \cos^2(h)$, or $\cos(h) = \pm \cos^2(2g)$. Then there exist h' which is a rational multiple of π such that $\cos(h') = \cos^2(2g)$ (precisely, if ‘‘+’’ in $\cos(h) = \pm \cos^2(2g)$ then define $h' = h$, if ‘‘-’’ then define $h' = h + \pi$). Now let b be a minimal positive integer for which $h'b, 2gb$ are both divisible by 2π , that is,

$$h'b = 2\pi a, \quad 2gb = 2\pi c, \quad (\text{S50})$$

for coprime (not necessarily mutually coprime) integers a, b, c . We then have

$$\frac{w^a + w^{-a}}{2} = \frac{(w^c + w^{-c})^2}{4} \quad (\text{S51})$$

where $w = e^{i\frac{2\pi}{b}}$. This is a polynomial in w with rational coefficients. Thus, all algebraic conjugates of w satisfy it as well. These algebraic conjugates are all primitive roots of unity of degree b , utilizing the fact that the cyclotomic

polynomial Φ_b is irreducible. We can then replace w to w^m where $\gcd(m, b) = 1$. As the right-hand-side of Eq. (S51) is non-negative, we get that $\cos(2\pi am/b) \geq 0$ for all m coprime to b .

When does this happen? Denote now $a = da_1$, $b = db_1$ where $d = \gcd(a, b)$ and $\gcd(a_1, b_1) = 1$. Let k be an arbitrary integer coprime with b_1 . Denote $m = k + Nb_1$ where N equals the product of the prime divisors of d which do not divide k . Now each prime divisor of d divides exactly one of the numbers k and Nb_1 , therefore it does not divide their sum m . Clearly m is also coprime with b_1 , and $\gcd(m, b) = 1$. Therefore $\cos(2\pi a_1 k/b_1) = \cos(2\pi a_1 m/b_1) = \cos(2\pi am/b)$ is non-negative. Next, $a_1 k$ takes all residues modulo b_1 which are coprime to b_1 . It follows that there are no residues coprime with b_1 in the interval $(b_1/4, 3b_1/4)$. Lemma 3 states that $b_1 \in \{1, 4, 6\}$, and so $\cos(h) = \cos(2\pi a/b) = \cos(2\pi a_1/b_1) \in \{0, 1/2, 1\}$. This then implies

$$\cos(2g) = \pm\sqrt{\cos(h)} \in \{0, \pm\sqrt{2}/2, \pm 1\}, \quad (\text{S52})$$

which further implies g is divisible by $\pi/8$. Hence, $g \notin \mathbb{Z}\pi/8$ yields irrational θ_1/π . ■

C. Lemma 3

Lemma 3. *Let n be a positive integer such that each number in the open interval $(n/4, 3n/4)$ is not coprime with n . Then $n \in \{1, 4, 6\}$.*

Proof. If $n = 2m + 1$ is odd, and $m \geq 1$, then $m \in (n/4, 3n/4)$. If $n = 4m + 2$ and $m > 1$, then $2m - 1 \in (n/4, 3n/4)$. If $n = 2$, then $1 \in (n/4, 3n/4)$. If $n = 4m$ and $m > 1$, then $2m - 1 \in (n/4, 3n/4)$. ■

- [1] R. Goodman and N. R. Wallach, *Representations and Invariants of the Classical Groups* (Cambridge University Press, 1998).
- [2] I. Marvian and R. W. Spekkens, A generalization of schur–weyl duality with applications in quantum estimation, *Communications in Mathematical Physics* **331**, 431–475 (2014).
- [3] D. A. Roberts and B. Yoshida, Chaos and complexity by design, *Journal of High Energy Physics* **2017**, 10.1007/jhep04(2017)121 (2017).
- [4] B. Bertini, P. Kos, and T. Prosen, Entanglement spreading in a minimal model of maximal many-body quantum chaos, *Phys. Rev. X* **9**, 021033 (2019).
- [5] R. Raussendorf and H. J. Briegel, A one-way quantum computer, *Phys. Rev. Lett.* **86**, 5188 (2001).
- [6] J. S. Cotler, D. K. Mark, H.-Y. Huang, F. Hernandez, J. Choi, A. L. Shaw, M. Endres, and S. Choi, Emergent quantum state designs from individual many-body wavefunctions, arXiv e-prints , arXiv:2103.03536 (2021), [arXiv:2103.03536 \[quant-ph\]](https://arxiv.org/abs/2103.03536).
- [7] B. Bertini, P. Kos, and T. Prosen, Exact spectral form factor in a minimal model of many-body quantum chaos, *Phys. Rev. Lett.* **121**, 264101 (2018).
- [8] J. Preskill, [Caltech lecture notes for physics 219/computer science 219 quantum computation course](http://theory.caltech.edu/~preskill/ph229/notes/chap6.pdf) (2020), <http://theory.caltech.edu/~preskill/ph229/notes/chap6.pdf>.
- [9] We mean this in two senses of the word: (i) The solutions hold for all g such that $g \notin \mathbb{Z}\pi/8$, i.e. for a *class* of models. (ii) The permutation operators $P(\pi)$ contain no ‘fine structure’, i.e. properties depending on the microscopic details of the system. Instead their only structure is ‘global’, namely that they permute the replicated spaces.
- [10] We credit the proof of this technical result to MathOverflow user Fedor Petrov of the V. A. Steklov Mathematical Institute in St. Petersburg.